Final Draft
of the original manuscript:

Avdeev, M.V.; Aksenov, V.L.; Tomchuk, O.V.; Bulavin, L.A.;
Haramus, V.M.; Osawa, E.:
**The spatial diamond-graphite transition in detonation
nanodiamond as revealed by small-angle neutron scattering**

The spatial diamond-graphite transition in detonation nanodiamond as revealed by small-angle neutron scattering

Mikhail V. Avdeev[1], Viktor L. Aksenov[1,2], Oleksandr V. Tomchuk[1,3], Leonid A. Bulavin[3], Vasyl M. Garamus[4], Eiji Ōsawa[5]

[1]Frank Laboratory of Neutron Physics, Joint Institute for Nuclear Research (FLNP JINR), Joliot-Curie 6, 141980 Dubna, Russia

[2]National Research Centre "Kurchatov Institute", Academician Kurchatov Square 1, 123182 Moscow, Russia

[3]National Taras Shevchenko University of Kyiv, Physics Department, Volodymyrska Str. 64, 01601 Kyiv, Ukraine

[4]Helmholtz-Zentrum Geesthacht, Centre for Materials and Coastal Research, Max-Planck-Str., D-215 02 Geesthacht, Germany

[5]NanoCarbon Research Institute, Asama Research Extension Centre, Shinshu University, Ueda, 386-8567 Nagano, Japan

E-mail: avd@nf.jinr.ru

Abstract A spatial transition of the carbon state in detonation nanodiamond (DND) from crystalline diamond inside the particle to a graphite-like state at DND surface is proposed on the basis of small-angle neutron scattering (SANS) analysis. The SANS contrast variation from concentrated (5 wt %) dispersions of DND in liquids (water, dimethylsulphoxide) reveals a shift in the mean scattering length density of DND as compared to pure diamond, which is related to the presence of a non-diamond component in the DND structure. At the same time, the diffusive character of the particle surface is deduced based on the deviation from the Porod law. The two observations are combined to conclude about the continuous radial density profile over the whole particle volume conforming to a simple power law. The profile naturally suggests that non-diamond states are concentrated mainly close to the particle surface; still there is no sharp boundary between the radial distributions of the two states of carbon in DND.

1. Introduction

The question how much the structural properties of nanocrystallites differ from the properties of bulk crystals is the key point of nanoscience [1-13]. Its origin is related to the fact that the binding configuration of atoms at the crystallite surface cannot fully repeat that of the

inside of the crystal, and, hence, there should be a transitional layer from a purely crystalline state of atoms inside the crystallite to a surface state. For nanoparticles with a highly specific surface such layer can comprise a significant part (up to 50%) of particle atoms resulting in principally new properties as compared to micron-sized crystals where the interface effects are small. One of the most remarkable examples of the discussed spatial transition is detonation nanodiamond (DND) with the crystallite size down to 5 nm [14-16]. It is characterized by a natural change of the sp^3 hybridization of carbon in the 3D diamond structure to the surface sp^2 graphite-like state [17,18]. The existence of the diamond lattice in 3D even at this limiting size scale is well supported by the X-ray diffraction (XRD) data [14-16]. At the same time, the sp^2 hybrid bonds are reflected in various spectroscopic (UV-Raman, XANES, FTIR) [19] and resonance (EPR, NMR) [20] methods. In some cases, the graphite-like shell comprising two-three graphene sheets is resolved directly in the HRTEM images [16].

Recently, the effective thickness of the non-diamond shell in DND was estimated [21] to be at the level of 0.5 nm (for the whole particle size of about 7 nm) from the data of small-angle neutron scattering (SANS) with the contrast variation on liquid dispersions of purified DND [15]. It was followed from the experimentally observed shift in the mean scattering length density (SLD) of DND over that of pure diamond towards lower values, which was explained by the fact that there is a significant difference in the mean SLD between diamond ($\rho_{diam} = 11.8(3) \times 10^{10} \, \text{cm}^{-2}$) and graphite ($\rho_{graph} = 7.0(3) \times 10^{10} \, \text{cm}^{-2}$). Then, the DND particles were assumed to be 'core-shell' structures with a sharp boundary between the diamond 'core' and graphite 'shell'. At the same time, a specific feature of DND additionally found by SANS is the diffusive character of the particle surface, which upsets the Porod asymptotic behavior of the scattering at large values of the momentum transfer and suggests a more complex modulation of the diamond-graphite spatial transition as compared to the 'core-shell' representation. Here, we show that a thorough consideration of this transition combining different scattering levels of the DND liquid dispersions gives an evidence for the existence of a continuous SLD profile over a whole DND particle. This means that the mentioned transition does not show any strict 'core-shell' boundary and formally starts from the particle center.

2. Experimental

For the analysis the reported previously [21] experimental SANS data for DND dispersions in water and dimethylsulphoxide (DMSO) are taken. The concentrated (10 wt %) solutions in H_2O and DMSO were synthesized by the stirred-media milling together with the

powerful sonication in wet conditions as described in [22]. During experiments on the SANS contrast variation the initial samples were diluted by half with different mixtures of light and heavy components of the solvents, so that the content of the deuterated solvent, η, in the final solutions took several values in the range of 0-50 vol. % at definitely one particle concentration. The choice of the η-range was motivated by the fact that at the used dilution of the initial solutions the particle concentration remained high to produce a rather strong SANS signal against the possible residual incoherent scattering background, which usually occurs in neutron scattering experiments (especially in case of hydrogen-containing solvents) after the raw data treatment. This has made it possible to achieve a rather good precision in the determination of the structural characteristics of DND clusters. Additionally, for the indicated η-range the coherent scattering from the solvents is low, which is important for describing the scattering from the diffusive surface of the particles (see discussion below).

The SANS curves within the q-interval of 0.05 - 2.5 nm^{-1} were obtained in accordance with the standard procedure at the SANS-1 instrument of HZG (Geesthacht, Germany). As it is followed from the previous analysis of the experimental data [21], DND nanoparticles in the liquid dispersions are associated into large (characteristic size above 120 nm) aggregates with a quite developed structure (fractal dimension about 2.3). The latter explains the interpenetration of the clusters and formation of gel-like structures in the concentrated solutions following from the dependence of the forward scattered intensity on the DND volume fraction. The absence of closed volumes in the clusters that are inaccessible for the solvent is concluded based on the characteristic changes of the scattering when varying the solvent SLD. The assumed structure of the clusters composed of DND nanoparticles in the studied solutions as 'seen' by SANS is schematically illustrated in Fig. 1. Possible structural details [17,23] concerning the non-sphericity of the DND particles (because of the polyhedral structure of crystallites) as well as their specific organization in clusters are omitted in Fig. 1, since they cannot be concluded unambiguously from the SANS curves.

3. Results and discussion

The changes in the experimental curves at different contents of deuterated components in the DND liquid dispersions are followed in Fig. 2. A monotonic decrease in the absolute scattered intensity with insignificant changes in the character of the curves is observed. The absence of secondary peaks and bands in the curves reflects the polydisperse nature of the DND particles, which smoothes the characteristic minima of the possible polyhedral DND structures and allows

one to consider them as spherical units. Two scattering levels are distinguished in the SANS curves in Fig. 2. They can be described in terms of the particle form-factor, $P(q)$, responsible for the inner structure of the basic DND particles (particle level at large q-values) and the structure-factor, $S(q)$, reflecting both the correlation between particles in the cluster and the correlation between clusters themselves (cluster level at small q-values). These factors are combined into the scattered intensity as:

$$I(q) = P(q)S(q) \qquad (1)$$

The $S(q)$ factor is responsible for the effective Guinier-type behavior of the scattering at the smallest q-value:

$$I(q) \underset{q<1/R_g}{\approx} I(0)\exp(-R_g^2 q^2/3), \qquad (2)$$

where $I(0)$ is the forward scattered intensity, and R_g is the apparent radius of gyration. Here these parameters are referred to the cluster level. At the given cluster concentration along with the characteristic cluster size these parameters are determined strongly by a specific radius of correlation between clusters [21]. In Fig. 2 the experimentally found radii of gyration of the cluster level are R_g = 18.3(1) nm for water and R_g = 16.1(3) nm for DMSO. It increases when diluting the systems. To some extent they depend on the preparation of the studied colloidal solutions, nevertheless, an essential observation is that for the given systems with one particle concentration this parameter does not change within the error with the contrast variation, thus indicating that the aggregates can be considered to be homogeneous at the scale > 10 nm, and the structure-factor $S(q)$ is certainly independent of the contrast. The break in the curves around q = 1 nm^{-1} is a trace of the Guinier law (2) but only for the particles composing clusters with the corresponding parameters $I_{ND}(0)$ and R_{gND} in Eq.2, which is modulated by the $S(q)$ factor of the clusters at smaller q-values. As an example, the extrapolation of the Guinier law for the particle level towards small q-values is shown in Fig. 2 for one of the samples of each series. The changes in $I_{ND}(0)$ and R_{gND} with the content of the deuterated components in the solvents are discussed below.

As one can see there are two regions with power-law dependence in the experimental curves (also distinguished in Fig. 2). The homogeneous character of the particles following from the contrast variation allows one to treat the two scattering levels in Fig. 2 by the unified exponential/power-law approximation [24]:

$$I(q) = G\exp\left(-q^2R_g^2/3\right) + B\exp\left(-q^2R_{gND}^2/3\right)\left(q^*\right)^{-P} +$$
$$+ G_{ND}\exp\left(-q^2R_{gND}^2/3\right) + B_{ND}\left(q_{ND}^*\right)^{-Ps} + C \qquad (3)$$

Again, the 'ND'-index denotes the particle (nanodiamond) level, while the parameters without indexes correspond to the cluster level; Ps corresponds to the particle surface; C is the residual incoherent scattering background. Each level in Eq.3 is represented by a combination of two terms, which are the purely Guinier-type term and the modified power-law type term. In the second term the renormalized q^*-variable ($q^* = q/[erf(kqR_g/\sqrt{6})]^3$, where k is an empirical constant equal to 1 for the mass scattering and 1.04 for the surface scattering) is used. The error function in the renormalization has a cut-off effect for the power-law term at small q-values, so one can apply the well-parameterized universal combination of the two terms in the simultaneous fitting of the experimental data comprising two types of the scattering. Additionally, when two levels are considered in one expression as in Eq.3, a specific exponential coefficient in the power-law term of the first level (here cluster level) is to be introduced to describe appropriately the transition between the two levels in a scattering curve. The similar approximation was used previously for treating the scattering from nanodiamond and other carbon nanostructures [21,25,26]. As a result, the parameters of both levels are obtained as a function of the content of the deuterated component in the solvent. While the power-law scattering of the cluster level with the exponent $P = 2.3$ reflects the fractal-type organization of the clusters, the particle level shows a power-law type scattering with the exponent of $Ps = 4.14$, which is different from the expected Porod exponent $Ps = 4$ for a sharp interface. Such kind of the q-dependence of the scattered intensity is a characteristic of the so-called diffusive interface [27-29]. The latter can be considered in two ways (Fig. 3).

First, the radially averaged SLD profile of the interface between two homogenous phases (particles and solvent) takes the form [27-29]:

$$\rho(r) = \begin{cases} \rho_0 - \rho_s, & 0 < r < R-d; \\ (\rho_0 - \rho_s)\left(\dfrac{R-r}{d}\right)^{\beta}, & R-d < r < R, \end{cases} \qquad (4)$$

where ρ_0 and ρ_s are the SLD of the particles and solvent, respectively; r is the distance from the center of the solute particle with the maximal outer radius of the shape, R, and d is the thickness of the transitional diffusive layer at the particle surface. In fact, the d-parameter characterizes the rate of the solvent penetration into the particle because of specific surface peculiarities (Fig. 3a). These peculiarities are determined by the β-exponent, which lies within

the interval of 0-1, so that the derivative of the $\rho(r)$ function has a limit $d\rho/dr \to \infty$ at a point $r = R$. The asymptotic behavior of the scattering form-factor for the profile (4) is [29]

$$P(q) \underset{q \to \infty}{=} Bq^{-(4+2\beta)} \tag{5}$$

where the B coefficient is defined as

$$B = 2\pi n(\rho_0 - \rho_s)^2 S\Gamma^2(\beta+1)/d^{2\beta} \tag{6}$$

and S is the area of the particle surface accessible for the solvent. In terms of Eq.3 the exponent $Ps = 4 + 2\beta$.

Another case is when spherical-like particles themselves have some inner non-homogeneous SLD distribution, and the solvent access is restricted by the outer particle radius, R (Fig. 3b). Then, ρ_0 is the SLD of some homogeneous particle "core", which starts to change towards the periphery at $r > R - d$ as:

$$\rho(r) = \begin{cases} \rho_0, & 0 < r < R-d; \\ \rho_0\left(\dfrac{R-r}{d}\right)^\beta, & R-d < r < R. \end{cases} \tag{7}$$

The principal difference with the previous case concerns the asymptotic behavior of the scattering for profile (7) when the particles are placed in the solvent with SLD ρ_s. The fact that there is no transitional interface between the particle and the solvent with one contrast factor for the profile (7) results in additional coherent scattering contributions from the solvent [30]. The asymptotic power-law type scattering is observed as well, but both the coefficient and the exponent of the corresponding power law are now affected strongly by the solvent SLD. However, there is a unique situation when Eqs. 5, 6 are true in the considered case as well. It takes place at $\rho_s = 0$.

From the two kinds of the diffusive profiles the profile (7) should be considered for nanodiamond particles after one takes into account their inhomogeneous structure with respect to a diamond-graphite spatial transition. Then, the ρ_0 density is naturally associated with the crystalline diamond in this case. However, to satisfy (5) the profile (7) follows the transition $\rho_{diam} \to 0$. If one adds the constant ρ_{graph} to (7) with the corresponding renormalization of ρ_0 to fix explicitly the required transition $\rho_{diam} \to \rho_{graph}$ at $r = R$, it will be equivalent to the situation $\rho_s \neq 0$ when Eq.5 does not hold. The contradiction is resolved, if $\beta \ll 1$ in (7), which really takes place in practice! In Fig. 4 one can compare the principal view of the SLD profile (7) for different d/R ratios with the profiles corresponding to the sharp Porod interface and mentioned

'core-shell' approximation with the transition $\rho_{diam} \to \rho_{graph}$, respectively. One can see that for a sufficiently small β-value the profiles (7) almost coincide with the sharp 'core-shell' interface at $r = R$ because of their infinite derivatives at the outer particle radius and, thus, describe well the transition to ρ_{graph}.

From the experimental viewpoint the closest case to the condition $\rho_s = 0$ corresponds to 0-10% of the deuterated component in the solvents, when $\rho_s = 0.13 \times 10^{10}\, cm^{-2}$ (10% of D_2O) and $\rho_s = -0.046 \times 10^{10}\, cm^{-2}$ (0% of D-DMSO) in water- and DMSO-based solutions, respectively. The slopes in the double logarithmic experimental plots in Fig. 2 for these solutions give for the β-parameter the value of 0.07(1) in accordance with Eq.5, so it satisfies well the condition $\beta \ll 1$. It grows a little with increasing content of the deuterated components in the solvents because of the effect of solvent scattering.

Like the 'core-shell' approximation the $\rho(r)$ function of kind (7) also has a break (at $r = R - d$) defined by the d-parameter, thus assuming a distinct boundary between the diamond core and the non-diamond diffusive shell. While such $\rho(r)$ explains the non-Porod behavior of the scattering at large q-values, one obtains surprisingly large d-values when fitting it to the experimentally found mean SLD of DND. Thus, for the 7-nm DND nanoparticle indicated in Fig. 1 in the monodisperse approximation the corresponding estimates give d = 2.5 nm. This means that for polydisperse particles (which, in fact, produce smeared scattering at the particle level in Fig. 2) a significant part of the particles should meet the condition $d = R$. This gives an idea to consider the corresponding approximation, or continuous diffusive profile (Fig. 4), as an intrinsic property of all particles. So, the substitution $d = R$ into (7) gives the formula:

$$\rho(r) = \rho_0 \left(1 - \frac{r}{R}\right)^\beta, \ 0 < r < R. \tag{8}$$

The smaller is the β-value, the lesser is the difference between (8) and (7). So, the smallness of the β-parameter allows one to consider the profile (8) as a good approximation to the profile (7) in the case when d is not strictly equal to R but approaches it (see Fig. 4).

The new radial profile suggests that there is no sharp boundary between the homogeneous "core" and diffusive layer, so a continuous transition from the ρ_0-value of the SLD in the particle center to zero value in the particle boundary takes place. Such approximation results in quite specific contrast behaviors of the scattering invariants corresponding to different parts of

the scattering curves. Thus, the forward scattered intensity is determined by the mean SLD of the profile (8), which is now can be easily found as

$$\bar{\rho} = \frac{1}{V} \int_0^R \rho(r) 4\pi r^2 dr = \frac{6\rho_0}{(\beta+1)(\beta+2)(\beta+3)} \tag{9}$$

where $V = (4/3)\pi R^3$ is the particle volume restricted by the radius R. The important point is that the mean SLD in this case does not depend on the particle size! So, despite the fact that the particles are polydisperse, from the viewpoint of the contrast variation they behave like monodisperse particles with the one mean SLD. Actually, in accordance with the definition of the effective match point, $\bar{\rho}_e$, for non-homogenous polydisperse particles [31] one has

$$\bar{\rho}_e = \langle \bar{\rho} V^2 \rangle / \langle V^2 \rangle = \bar{\rho}. \tag{10}$$

Hereafter, the brackets $\langle ... \rangle$ denote the averaging over the polydispersity function.

In the standard procedure of the contrast variation one finds $\bar{\rho}$ from the dependence of the forward scattered intensity $I_{ND}(0)$ (referred to the particles) on the varied solvent SLD. Here, for this purpose it is preferable to use the cluster level, i.e. the effective forward scattered intensity from the clusters. In accordance with (1) two kinds of the forward scattered intensity differ only by the $S(0)$ factor, which does not depend on the contrast. So, as it follows from the general equation for polydisperse formations [31] the forward scattered intensity of the clusters depends on the contrast $\bar{\rho} - \rho_s$ as

$$I(0) = \left(n(\bar{\rho}_e - \rho_s)^2 \langle V^2 \rangle + n \langle (\bar{\rho} - \bar{\rho}_e)^2 V^2 \rangle \right) S(0) = n(\bar{\rho} - \rho_s)^2 \frac{16\pi^2}{9} \langle R^6 \rangle S(0) \tag{11}$$

The cluster level gives much better precision ($< 5\%$) in the determination of $I(0)$ as compared to the particle level because the former is strongly affected by the scattering from the clusters, and some effect of the residual background cannot be excluded either. The same problems concern another Guinier parameter of the particles, R_{gND}, which was found to be 3.0(5) nm for both kinds of solutions and whose precision does not make it possible to follow reliably its change with the contrast variation.

The concluded contrast dependence in (11) is verified in the experiment (see the insets to Fig. 2), where a strongly linear behavior of the parameter $\sqrt{I(0)}$ (linear regression coefficients are –0.992 and –0.999 for water and DMSO, respectively) depending on the content of the deuterated component in both solvents is observed. It gives the match points (and, as a consequence, $\bar{\rho}$-values) in the intersection of the fitting line with the abscissa axis (denoted by

the arrows in the insets to Fig. 2 for the two solutions). The mean SLD values found in this way (experimental match points) $\bar{\rho} = 10.5(5) \times 10^{10} \, \text{cm}^{-2}$ (for water) and $\bar{\rho} = 10.2(4) \times 10^{10} \, \text{cm}^{-2}$ (for DMSO) agree well with the value $\bar{\rho} = 10.4(3) \times 10^{10} \, \text{cm}^{-2}$ estimated from (9) by using the known SLD of diamond, $\rho_0 = \rho_{diam}$, and experimentally found β. Thus, one has very good consistency of the continuous profile (8) reflecting the diffusive character of the particle surface with the mean particle SLD, which is not properly achieved, if one uses the 'core-shell' approximation.

A simplified profile (8) makes it possible to estimate easily the rate of the particle polydispersity. For the particle level it gives:

$$I_{ND}(0) \approx n\bar{\rho}^2 \frac{16\pi^2}{9} \langle R^6 \rangle, \tag{12a}$$

$$R_{gND}^2 \approx \frac{12}{(\beta+4)(\beta+5)} \frac{\langle R^8 \rangle}{\langle R^6 \rangle}, \tag{12b}$$

$$B \approx 8\pi^2 n\rho_0^2 < R^{2-2\beta} > \Gamma^2(\beta+1). \tag{12c}$$

In (12c), as compared to (6), the B-coefficient is given for $\rho_s = 0$, and the explicit relation between S and R for the spherical particles is also taken into account. So, the experimentally found values of the scattering invariants (12) in the case of the 10% and 0% content of the deuterated water and D-DMSO in the solvent, respectively, can be used to calculate various moments of the R-distribution function. Then, assuming the log-normal type of the latter, one finds its parameters, which are the most probable radius, R_0, and the mean squared deviation of the logarithm of the radius, σ, which finally are $R_0 = 1.36(5)$ nm, $\sigma = 0.40(1)$ for water and $R_0 = 1.40(3)$ nm, $\sigma = 0.39(1)$ for DMSO.

4. Conclusions

To summarize, the SANS contrast variation on the associates of the nanodiamond particles evidences a continuous transition from diamond inner states to graphitic surface states over the whole crystallite volume of DND. It can be parameterized in terms of the power-law type (8). This is consistent to some extent with the data of *ab initio* computer simulations [32,33] for diamond nanocrystals (size up to 3.3 nm) which show that the most stable structures require the existence of transitional sp^{2+x} bonds over the crystalline volume. They are concentrated preferably at the edges of the crystal with its growth matching different orientational configurations of the polyhedron facets of nanocrystallites. The spherical 'core-shell'

representation of the DND particle can be considered as an approximation to the continuous density profile, which gives a reasonable thickness of the non-diamond shell of about 0.4 nm. It reflects the natural fact that significant deviations from the purely diamond structure are mostly concentrated close to the DND surface. This feature makes the revealed density profile consistent with the XRD data. The diamond lattice distortions in the central part of the crystallites are small to cause observable deviations in the corresponding positions of comparatively wide (because of the small particle size) XRD peaks. At the same time, the principally broader transition from diamond to graphite than in the case of the 'core-shell' structure explains well why XRD gives effectively smaller diamond crystallite size as compared to the SANS data [21].
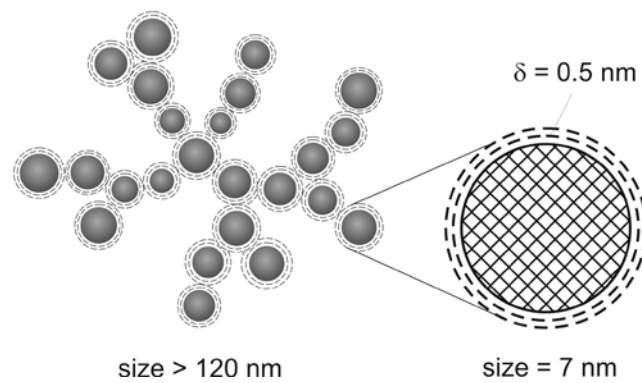
Acknowledgments

Fig. 1. Schematic view of a developed DND cluster (as concluded in [21]) in liquid dispersions with the representation of its basic structural unit – DND particle composed of a crystalline diamond 'core' and a graphene-like 'shell' (from the data of the SANS contrast variation treated with the 'core-shell' approximation). Both levels are shown as 'seen' by SANS illustrating the main averaged features revealed by the method.
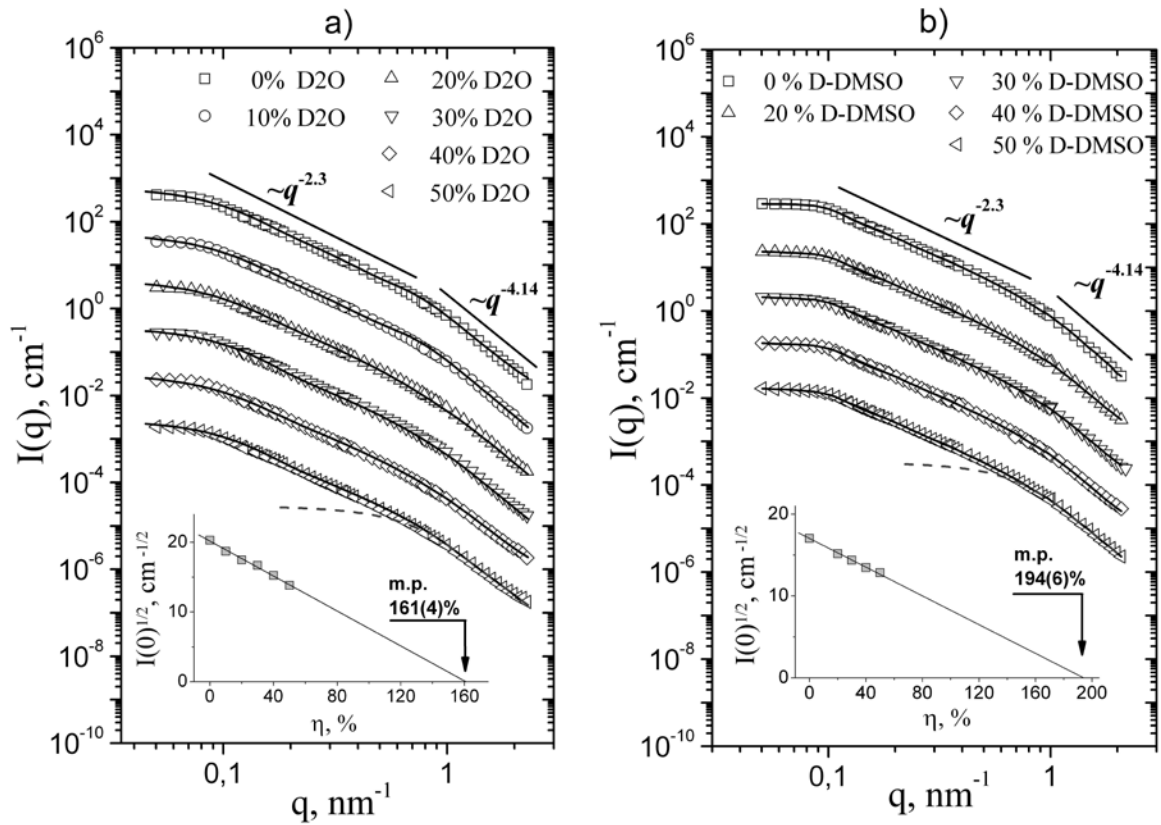
Fig. 2. Experimental SANS curves for 5% DND dispersions in water (*a*) and DMSO (*b*) at different contents of the deuterated components in the solvents. For a convenient view each curve in both graphs (starting from 10% of the deuterated component in the solvent) is divided by 10 as compared to the previous one. The fitting solid lines correspond to the unified exponential/power-law approximation [24]. The power-law scattering types for the cluster level (small *q*-values) and particle level (large *q*-values) are distinguished. As an example, the exponential/power-law approximation to the particle scattering level is shown (dashed line) for the lowest curves. The insets show the dependences of the $(I(0))^{1/2}$ parameter (found from the fits to the scattering curves) on the volume fraction of the deuterated component in the solvent, η; solid lines are linear fits, which intercept the η-axis in the match points denoted by arrows.
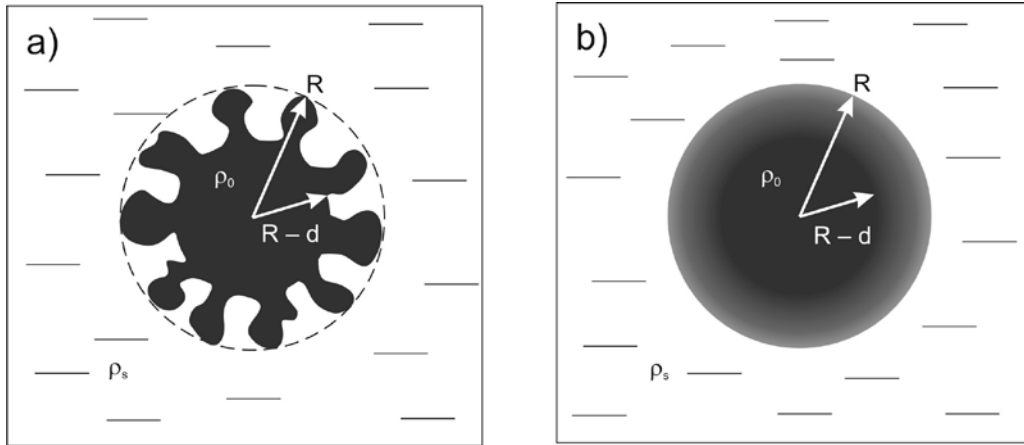
Fig. 3. Conventional representation of two kinds of particles with diffusive surface.
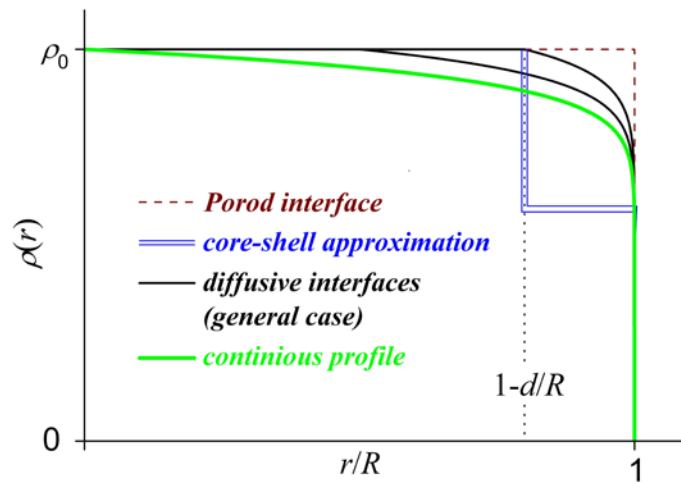

Fig. 4. Considered SLD profiles in spherical-like DND particles. For diffusive interfaces including continuous profile $\beta = 0.07 \ll 1$. Two diffusive interfaces for the general case (black lines), Eq.7, with different d are shown to demonstrate that the larger is d the closer is the profile to the continuous one (green line), Eq. 6. ρ_0 corresponds to the SLD of diamond. The SLD of the shell in the 'core-shell' approximation corresponds to the SLD of graphite.

References

[1]   Poole Ch P, Frank Jr and Owens J 2003 *Introduction to nanotechnology,* 3rd edition (Wiley-Interscience)

[2]   Roduner E 2006 *Chem. Soc. Rev.* **35** 583−592

[3]   Kodama R H, Berkowitz A E, McNiff Jr. E J and Foner S 1996 *Phys. Rev. Lett.* **77** 394−397

[4]   Wautelet M 2004 *J. Phys.: Condens. Matter* **16** L163−L166

[5]   Sun C Q, Pan L K, Li C M and Li S 2005 *Phys. Rev. B* **72** 134301

[6]   Qi W H, Wang M P, Zhou M and Hu W Y 2005 *J. Phys. D: Appl.* **38** 1429−1436

[7]   Yang C C and Li S 2007 *Phys. Rev. B* **75** 165413

[8]   Richman E K and Hutchison J E 2009 *ACS Nano* **3** 2441−2446

[9]   Wautelet M and Duvivier D 2007 *Eur. J. Phys.* **28** 953−959

[10]   Ouyang G, Li X L, Tan X and Yang G W 2007 *Phys. Rev. B* **76** 193406

[11]   Seyed-Razavi A., Snook I K and Barnard A S 2010 *J. Mater. Chem.* **20** 416−421

[12]   Guisbiers G 2011 *J. Phys. Chem. C* **115** 2616−2621

[13]   Maugeri L, Iadecola A, Joseph B, Simonelli L, Olivi L, Okubo M, Honma I, Wadati H, Mizokawa T and Saini N L 2012 *J. Phys.: Condens. Matter* **24** 335305

[14]   Shenderova O A, Zhirnov V V and Brenner D W 2002 *Crit. Rev. Solid State Mater. Sci.* **27** 227−356

[15]   Ōsawa E 2008 *Pure Appl. Chem.* **80** 1365−1379

[16]   Alekseenskii A E, Baidakova M V, Vul' A Y and Siklitskii V I 1999 *Phys. Solid State* **41** 668−671

[17]   Raty J Y, Galli G, Bostedt C, Buuren T W and Terminello L J 2003 *Phys. Rev. Lett.* **90** 37402

[18]   Eidelman E D, Siklitsky V I, Sharonova L V, Yagovkina M A, Vul' A Y, Takahashi M, Inakuma M., Ozawa M and Ōsawa E 2005 *Diamond Related Mater.* **14** 1765−1769

[19]   Osswald S, Yushin G, Mochalin V, Kucheyev S O and Gogotsi Y. 2006 *J. Am. Chem. Soc.* **128** 11635−11642

[20]   Panich A M, Shames A I, Vieth H -M, Takahashi M, Ōsawa E and Vul' A Y 2006 *Eur. Phys. J. B* **52** 397−402

[21]   Avdeev M V, Rozhkova N N, Aksenov V L, Garamus V M, Willumeit R and Ōsawa E 2009 *J. Phys. Chem. C.* **113** 9473−9479

[22] Krüger A, Kataoka F, Ozawa M, Fujino T, Suzuki Y, Aleksenskii A E, Vul' A Y and Ōsawa E 2005 *Carbon* **43** 1722–1730

[23] Barnard A S 2008 *J. Mater. Chem.* **18** 4038–4041

[24] Beaucage G 1996 *J. Appl. Cryst.* **29** 134–146

[25] Avdeev M V, Tropin T V, Aksenov V L, Rosta L, Garamus V M and Rozhkova N N 2006 *Carbon* **44** 954–961

[26] Avdeev M V, Aksenov V L and Rosta L 2007 *Diamond Relat. Mater.* **16** 2050–2053

[27] Schmidt P W 1995 In *Modern aspects of small-angle scattering* (Brumberger H (Ed), Kluwer Academic Publishers: Netherlands)

[28] Schmidt P W 1989 In *The Fractal Approach to Heterogeneous Chemistry* (Avnir D (Ed), John Wiley & Sons: Great Britain)

[29] Schmidt P W, 1991 *J. Appl. Cryst.* **24** 414–435

[30] Heinemann A, Hermann H, Wiedenmann A, Mattern N and Wetzig K 2000 *J. Appl. Cryst.* **33** 1386–1392

[31] Avdeev M V 2007 *J. Appl. Cryst.* **40** 56–70

[32] Barnard A S, Russo S P and Snook I K 2004 *Diamond Relat. Mater.* **12** 1867–1872

[33] Barnard A S and Sternberg M 2007 *J. Mater. Chem.* **17** 4811–1819